Radiation Physics and Chemistry 180 (2021) 109231

Contents lists available at ScienceDirect

Radiation Physics and Chemistry

journal homepage: www.elsevier.com/locate/radphyschem

EPR response of anhydrite crystal ($CaSO_4$) for dosimetry of gamma photon beams

Nilo F. Cano [a,*], T.K. Gundu Rao [b], Jorge S. Ayala Arenas [b], Henry S. Javier-Ccallata [c], S. Watanabe [d]

[a] Instituto do Mar, Universidade Federal de São Paulo, Rua Doutor Carvalho de Mendonça, 144, CEP 11070-100, Santos, SP, Brazil
[b] Escuela Profesional de Física, Facultad de Ciencias Naturales y Formales, Universidad Nacional de San Agustín de Arequipa (UNSA), Av. Independencia S/N, Arequipa, Peru
[c] Facultad de Ciencias e Ingeniería, Universidad Tecnológica del Perú (UTP), Av. Tacna y Arica 160, Arequipa, Peru
[d] Instituto de Física, Universidade de São Paulo, Rua do Matão, Travessa R, 187, CEP 05508-090, São Paulo, SP, Brazil

ARTICLE INFO

Keywords:
Anhydrite ($CaSO_4$)
Radiation dosimetry
EPR

ABSTRACT

An anhydrite ($CaSO_4$) natural sample was studied as possible dosimeter for low and high gamma doses using the technique of electron paramagnetic resonance (EPR). EPR spectrum showed signals due to $(SO_3)^-$, $(SO_4)^-$ radicals and O^- center. The anhydrite sample was irradiated with gamma rays with low-dose ranges typical for medical therapy (1–20 Gy) up to high-dose of about 70 kGy. The EPR centers due to $(SO_3)^-$ and $(SO_4)^-$ exhibited a linear dose response in the dose range from 1 Gy to 500 Gy, whilst the O^- center presented a supra-linear dose response in the range of 50 to 5 kGy.

1. Introduction

Many natural and synthetic solid materials are already well known and used in luminescence dosimetry applications due to their high sensitivities, low detectable minimum doses, wide linearity ranges, and high saturation levels (McKeever et al., 1995; Preto et al., 2017; Cano et al., 2008, 2015; Watanabe et al., 2015a, 2015b; Barbosa et al., 2014). However, there are only a few well-established solid materials for electron paramagnetic resonance (EPR) dosimetry.

The solid-state dosimetry using the EPR technique was established and developed during the last 50–60 years (Bradshaw and Cadena, 1962). According to Ikeya (1993), the energy of ionizing radiation produces defects in the solid, the number of defects produced is proportional to the dose of radiation absorbed by the solid. Some of these defects are paramagnetic, and their number, related to the dose, can be measured using the EPR technique.

Since the EPR started to be applied to the dosimetry of ionizing radiation, different natural or synthetic materials have been proposed as dosimeters (Chen et al., 2007; Lund et al., 2002, 2005; Murali et al., 2001; Olsson et al., 2000). Perhaps one of the most representative materials for EPR dosimetry is alanine, mainly for high doses. The EPR/alanine method has proven its relevance for radiosurgery (Tuta et al., 2020), radiotherapy (Marrale et al., 2015, 2016), brachytherapy (De Angelis et al., 1999), X-ray beam measurements (Nasreddine et al., 2020), dosimetry in a mixed neutron and gamma radiation field (Trompier et al., 2004) and among other applications (Baffa and Kinoshita, 2014). However, due to its complicated EPR spectrum that includes three different radicals (Malinen et al., 2003a, 2003b; Heydari et al., 2002; Sagstuen et al., 1997), and despite having a sensitivity with relative precision that allows evaluating radiation doses lower than 2 Gy (Ciesielski et al., 2003), the alanine is far from being an ideal EPR dosimeter. On the other hand, there are new materials with potential application in EPR dosimetry. Among the new materials for EPR dosimetry are organic and inorganic substances such as glucose (Belahmar et al., 2018), strontium sulfate (Acar et al., 2016), phenolic (Gallo et al. 2017a, 2017b; Smith et al., 2017), ammonium oxalate (Rushdi and Beshir, 2019), sulfamic acid, sulfanillic acid, homotaurine, and taurine (Alzimami et al., 2014), and between others, which show that the EPR technique together with these materials can provide reliable dosimeters in different areas of dosimetry. For this reason, attempts to synthesize new materials or the use of natural materials for radiation dosimetry by EPR is continuous, and requires further study of their

* Corresponding author.
E-mail addresses: nilo.cano@unifesp.br, nilocano@if.usp.br (N.F. Cano), tgundu@unsa.edu.pe (T.K. Gundu Rao), jayala@unsa.edu.pe (J.S. Ayala Arenas), c16698@utp.edu.pe (H.S. Javier-Ccallata).

https://doi.org/10.1016/j.radphyschem.2020.109231
Received 4 June 2020; Received in revised form 9 September 2020; Accepted 12 October 2020
Available online 6 November 2020
0969-806X/

dosimetric properties.

Some carbonates with chemical composition similar to anhydrite have been extensively studied using electron paramagnetic resonance (EPR) for applications in dosimetry (Bortolin and Onori, 2005; Murali et al., 2001; Onori et al., 1998), and in archaeological and geological dating (Watanabe et al., 2016, 2019; Cano et al., 2019). However, no published papers in the literature were found related to study of natural anhydrite crystal as a possible EPR dosimeter. In this context, this paper reports the characterization of natural anhydrite as a promising material for dosimetric applications. We performed the investigations on the behavior and sensitivity of EPR signals with dose, dose linearity, reuse temperature, and fading properties to develop a new material possibly suitable for dosimetry applications.

2. Materials and methods

Anhydrite ($CaSO_4$) crystal was purchased from stone dealer, LEGEP Minerals Ltd, Brazil, who imported the material from Peru in the form of large fragment of pale blue color crystals.

The anhydrite sample was crushed and sieved retaining grains with diameters between 0.080 and 0.180 mm for EPR measurements.

Irradiation of the material with gamma radiation was carried out using two ^{60}Co gamma sources installed at the Radiations Technology Center (CTR) of the Institute for Energy and Nuclear Researches (IPEN). Irradiations for low dose of the order of Gy were done using a panoramic type source with a dose rate of 7.88 Gy/h at sample position. For high doses in the region of hundreds of Gy to kGy were done using a source type gamma-cell with a dose rate of 0.64 kGy/h. Anhydrite samples were irradiated in air and the radiation doses delivered to the samples ranged from 1 Gy to 70 kGy. Samples were irradiated at room temperature and under electronic equilibrium conditions, and the radiation doses delivered to the samples ranged from 1 Gy to 70 kGy. During the irradiation, anhydrite samples were placed in polymethyl methacrylate (PMMA) holders.

EPR spectra of the powdered anhydrite sample were obtained at room temperature utilizing a MiniScope MS-5000 spectrometer from Freiberg Instruments, using a standard rectangular cavity in the range of X-band (9.1417 GHz), 20 mW microwave power, field modulation of 0.2 mT at 100 kHz, and a sweep time of 120 s. These parameters were optimized through preliminary analysis to acquire a good signal and to avoid saturation and distortion of the form of the anhydrite EPR spectrum. Powder samples were filled in quartz capillary tubes and placed inside the EPR cavity, using a mass of 100,0 ± 0,1 mg. The spectrometer was warmed up to at least 1 h before starting the measurements.

3. Results and discussion

In a paper published in J. Lumin. (Cano et al., 2020), the EPR spectrum of an anhydrite sample previously heat-treated at 500 °C for 30 min and then irradiated with 5 kGy gamma rays (Fig. 1) was presented. The spectrum is composed of six signals, labeled as center I, II, III, IV, V and VI. Centers I, V, and VI are prominent, well defined, and without overlap between them.

Cano et al. (2020) identified all these signals and the center I with principal g-values $g_{||} = 2.011$ and $g_{\perp} = 2.012$ was assigned to $(SO_4)^-$ radical. Centers II, III and IV are characterized by axial g-tensors and all these three centers were also attributed to $(SO_4)^-$ radicals (Cano et al., 2020). On the other hand, center V with an isotropic g-value equal to 1.9953 was attributed to the formation of isotropic sulfur tri-oxide anion $(SO_3)^-$ (Cano et al., 2020). Finally, the center VI characterized with an isotropic g factor 2.015 is due to an intrinsic O^- type center (Cano et al., 2020).

Before studying the dosimetric properties of anhydrite crystal such as reproducibility, stability and dose dependence of EPR signals, the effect of microwave power and modulation amplitude were investigated. The microwave power is one of the main parameters affecting the EPR

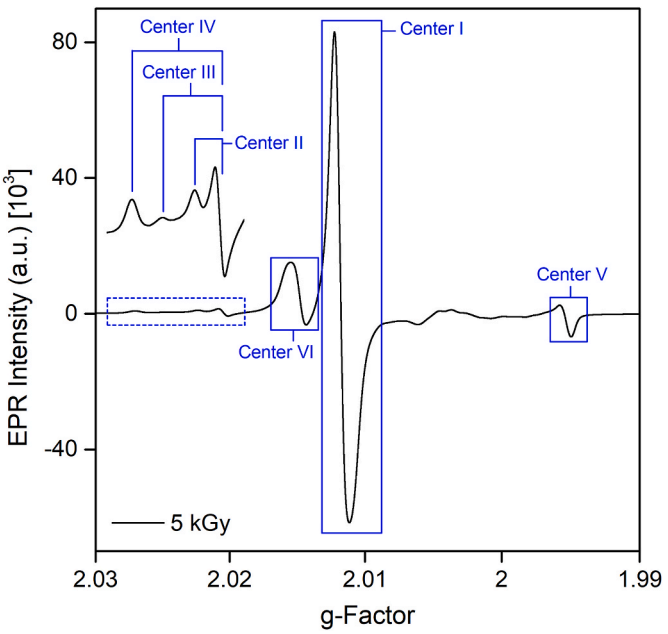

Fig. 1. Room temperature EPR spectrum of gamma irradiated anhydrite (5 kGy) (from Cano et al., 2020).

measurements. Fig. 2 shows the EPR signal intensity as a function of the square root of the microwave power at room temperature for the anhydrite around g=2.011 (center I). The EPR intensity increases with the square root of the microwave power up to at least 40 mW without saturation. In this work, measurements were performed with a microwave power of 20 mW in order to increase the signal-to-noise ratio, without entering the saturation region of the EPR signals. Saturation was found to occur at about 60 mW microwave power. Fig. 3 shows the intensity of EPR signal as a function of the modulation amplitude in a range from 0.04 up to 1.4 mT. The intensity values were normalized to their maximum. The EPR intensity increases with modulation amplitude in the entire modulation range analyzed even though the intensity

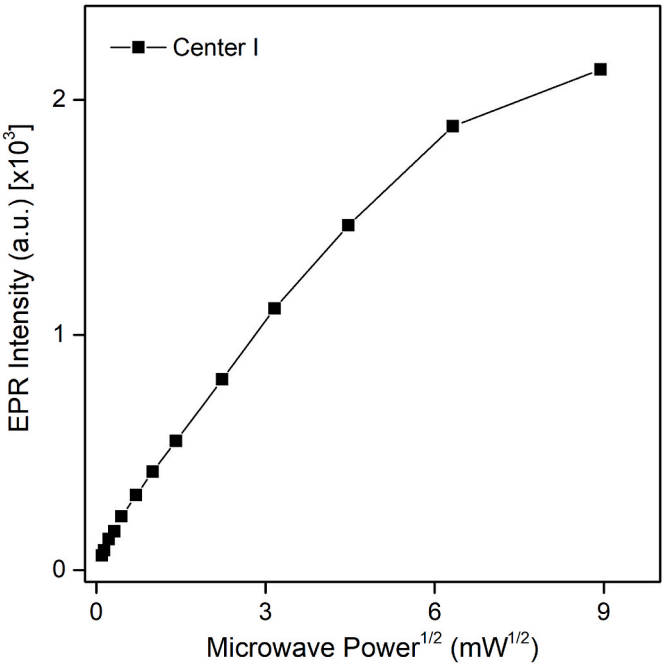

Fig. 2. Variation of EPR intensity vs. square root of microwave power.

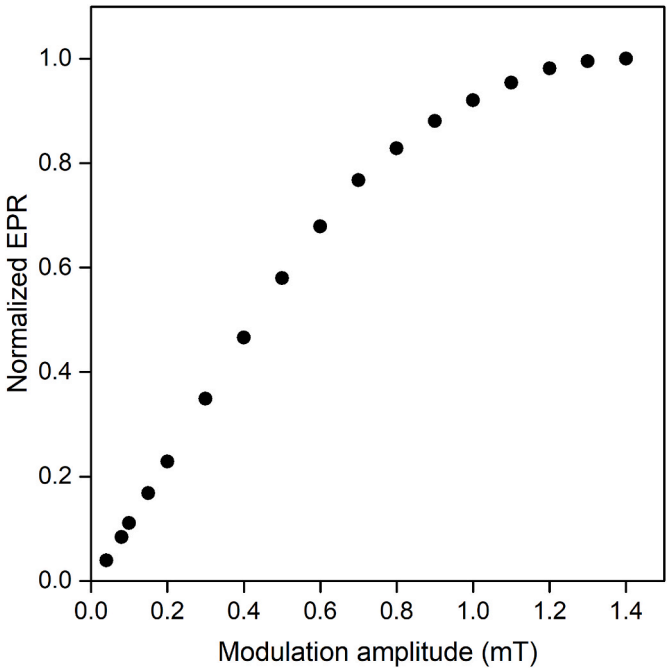

Fig. 3. Variations of EPR signal intensities with applied modulation field for the anhydrite sample.

growth is linear up to 0.6 mT and tend to saturate at 1.0 mT. We chose the modulation amplitude of 0.2 mT because it is in the linear region and with this value, we found a good compromise between signal enhancement and negligible large spectrum distortions.

Reproducibility of the EPR signals of anhydrite sample was verified utilizing two groups of five samples. The samples of the two groups were submitted five times to the same procedure of thermal treatment at 500 °C for 30 min (defined for reutilization) followed by irradiation. The first group was irradiated with 1 Gy and the second group with 5 kGy. Fig. 4 shows the reproducibility of center I EPR signal for the group irradiated with a dose of 1 Gy. This result shows a maximum standard deviation of 3,2%. On the other hand, for the samples of the second group, a maximum standard deviation of 1.2% was obtained. These results show that the anhydrite sample has a high reproducibility in its EPR signals after successive heat treatments and irradiations between 1 Gy up to 5 kGy.

EPR centers stability was measured using the isochronal thermal method at various temperatures. In this method, the sample is heated up to a given temperature, maintained there for 10 min and then rapidly cooled down to room temperature. The results of the thermal annealing behavior of the EPR centers of the anhydrite crystal are presented in Fig. 5. It is observed that center I with nearly isotropic g-tensor start reducing their intensity from 170 °C and decay completely at about 270 °C. On the other hand, it is observed that the center V isolated by the other EPR centers in the EPR spectrum, decay in the temperature region of 220 to 360 °C. Finally, the center VI is observed to become unstable at about 240 °C and subsequently decays in the temperature range 240 - 320 °C.

The EPR signal stability of the radiation-induced centers in gamma-irradiated anhydrite crystals (pre-annealed at 500 °C for 30 min and then exposed to a γ-dose of 5 kGy) with time after irradiation was also studied. After irradiation, sample was kept at room temperature in plastic bags and stored in the dark. The EPR spectrum of this sample was recorded several times during a period of four months after irradiation at the same spectrometer settings and the same room temperature (23 ± 2 °C) and relative humidity (around 35%) conditions. The EPR measurements remained within 2,5% of the original measurement during the four months period. This result shows no signal fading upon long-time storage and proves the high stability of all EPR signals of anhydrite crystal.

Both stability results of the EPR centers with temperature and with time show that centers I, V and VI are very stable at room temperature, and therefore suitable for possible use of anhydrite crystal in radiation dosimetry.

Once these preliminary studies were performed, the dose response of centers I, V, and VI was investigated.

Figs. 6 and 7 show the EPR spectra of anhydrite crystal irradiated with gamma doses from 1 Gy to 70 kGy (source of ^{60}Co) after the previous thermal annealing mentioned above. The EPR signal of center I

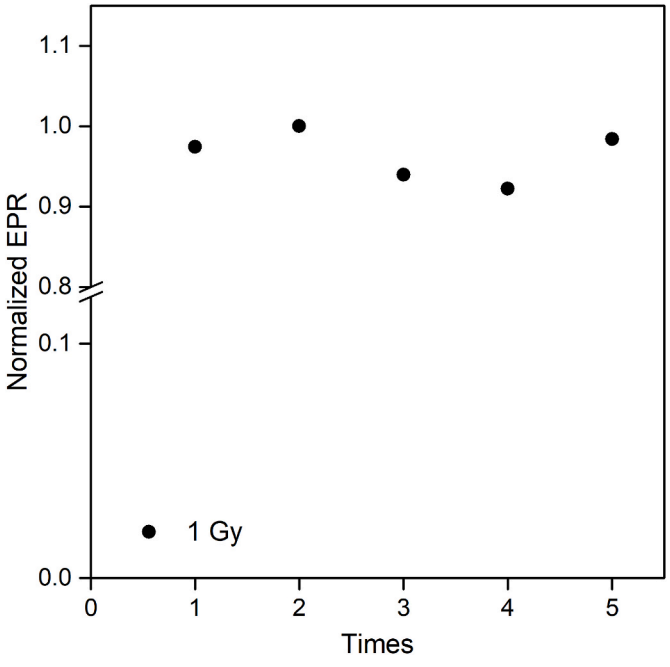

Fig. 4. Anhydrite sample EPR response reproducibility: dose 1 Gy of ^{60}Co gamma radiation.

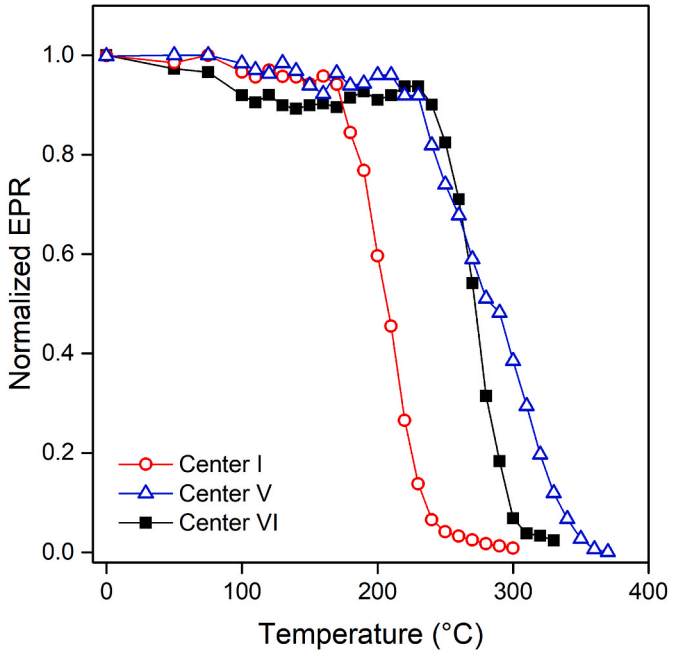

Fig. 5. Isochronal-thermal decay curves of the centers I, V and VI.

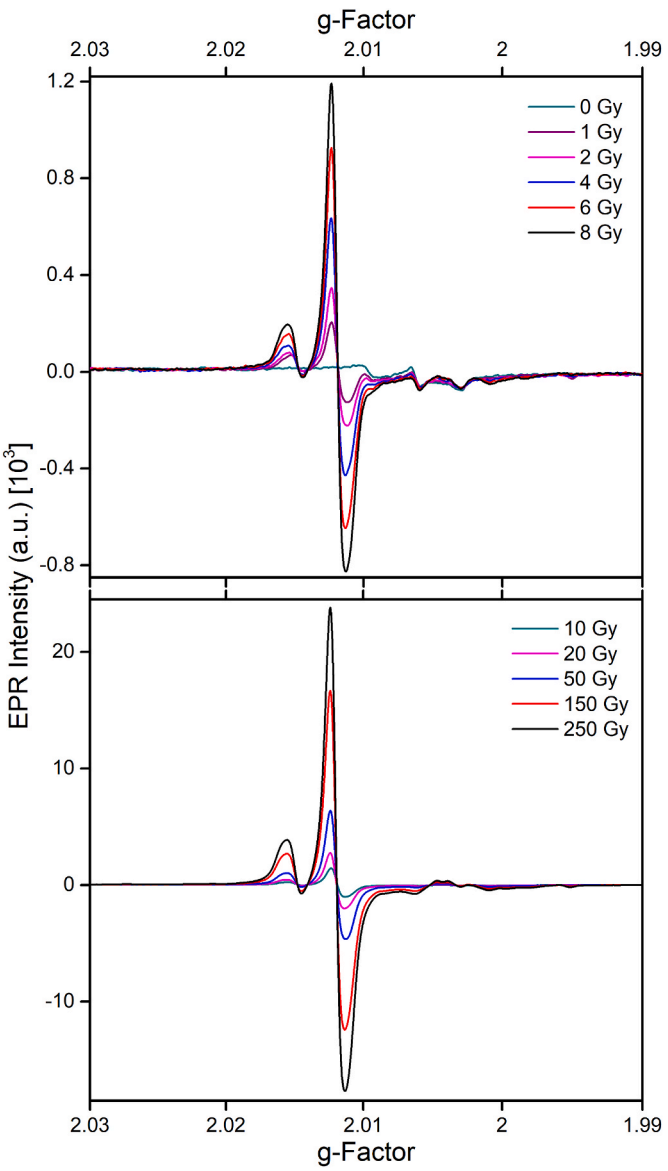

Fig. 6. The EPR spectra of the anhydrite samples irradiated to different doses between 1 Gy and 250 Gy.

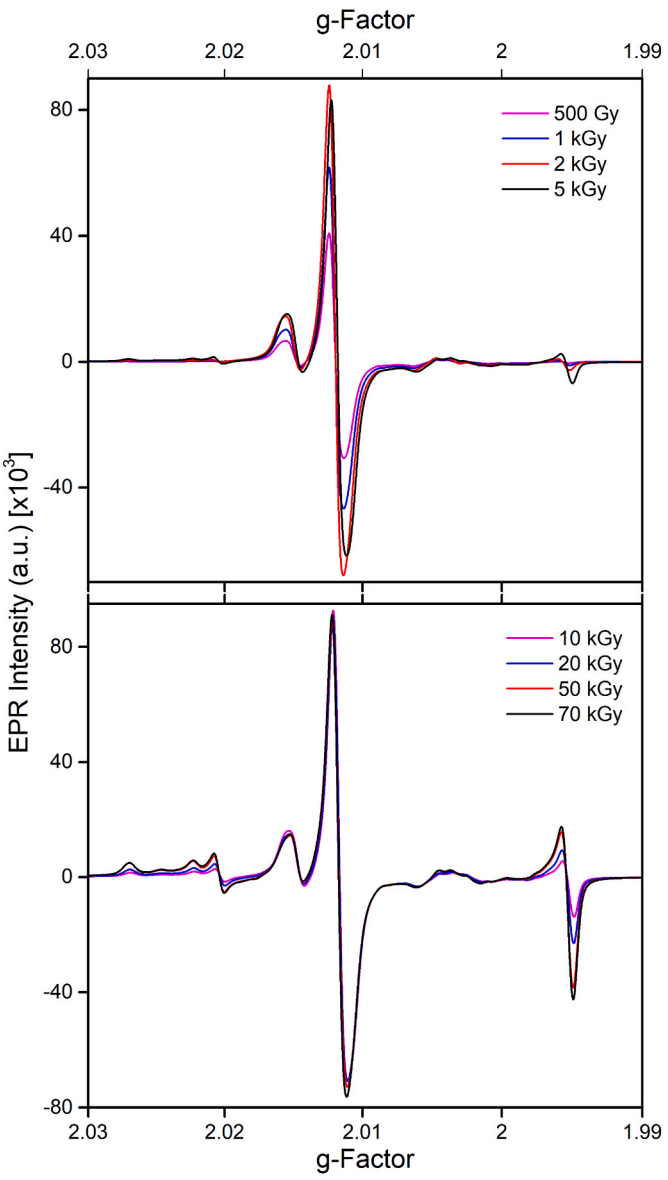

Fig. 7. The EPR spectra of the anhydrite samples irradiated to different doses between 500 Gy and 70 kGy.

always appear more intense than the other EPR signals, even for higher doses. Centers II, III and IV only appear for doses above 500 Gy and have a high overlap between them, while centers I and VI are induced with gamma radiation for doses of 1 Gy (see Fig. 6). On the other hand, center V is induced for doses from 50 Gy (Fig. 6). These results indicate that the anhydrite crystal can detect radiation-induced signals even much less than 1 Gy, as can be seen in Fig. 6.

Figs. 8 and 9 shows the EPR intensity of the I, V and VI centers as a function of gamma irradiation dose. Each point represents the peak-to-peak intensity of the EPR signal.

Fig. 8 shows the EPR response of the centers I and VI as a function of ^{60}Co γ-ray radiation doses between 1 and 10 kGy. Analyzing the dose response curves with log axes in the same scale, as shown in Fig. 8, it can be observed that the EPR response of both centers has a linear behavior in the dose range of 1 Gy to 500 Gy and then the response shows saturation. The response of center V with g = 1.9953 is supra-linear for doses between 50 and 5 kGy and saturates thereafter (Fig. 9). For low doses of less than 50 Gy, center V of the anhydrite is not very sensitive. In this manner, the entire EPR vs. dose curve of the center V can be used for dosimetry from 10 Gy up to high-dose of 5 kGy.

All these results show the usefulness of anhydrite sample for dosimetry for dose between 1 Gy and 5 kGy, with enormous cost advantages in relation to other traditional detectors. In this case fading requires no attention. Anhydrite sample may even be reutilized, with a very simple heat treatment of 500 °C for 30 min. Therefore, anhydrite is a very low cost, promising and reliable dosimetric material.

4. Conclusion

The EPR spectra of anhydrite sample heat treated at 500 °C for 30 min and irradiated with different gamma doses present five signals due to $(SO_4)^-$ and $(SO_3)^-$ radicals and the O^- type center. The linear and supra-linear behavior to gamma radiation of the three EPR centers of the anhydrite, characterized by having a simple spectrum without overlap, high repeatability and stability, and a reuse temperature of 500 °C for 30 min, favor the usefulness of anhydrite crystal as a promising dosimeter for doses from 1Gy to 5 kGy. The three-radiation sensitive EPR signals demonstrate that anhydrite could be of significant importance to researchers in a wide variety of fields related to dosimetry.

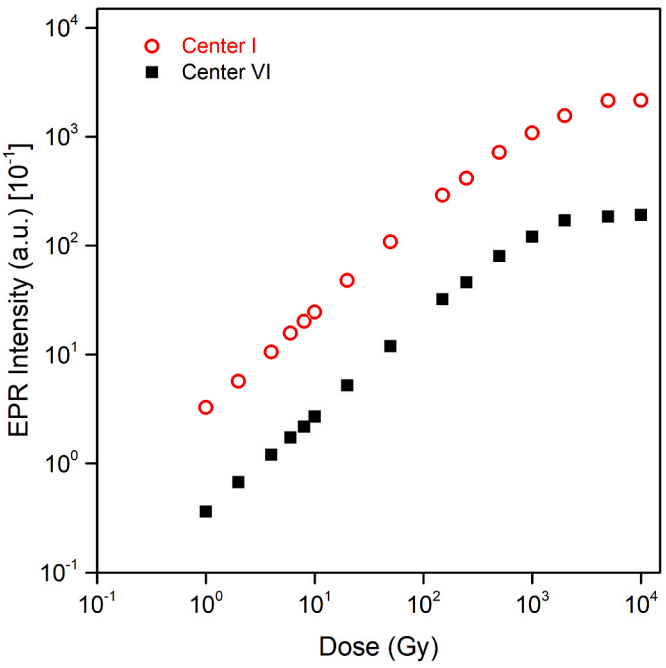

Fig. 8. Dose response curve of centers I and VI irradiated with gamma ray between 1 Gy and 10 kGy.

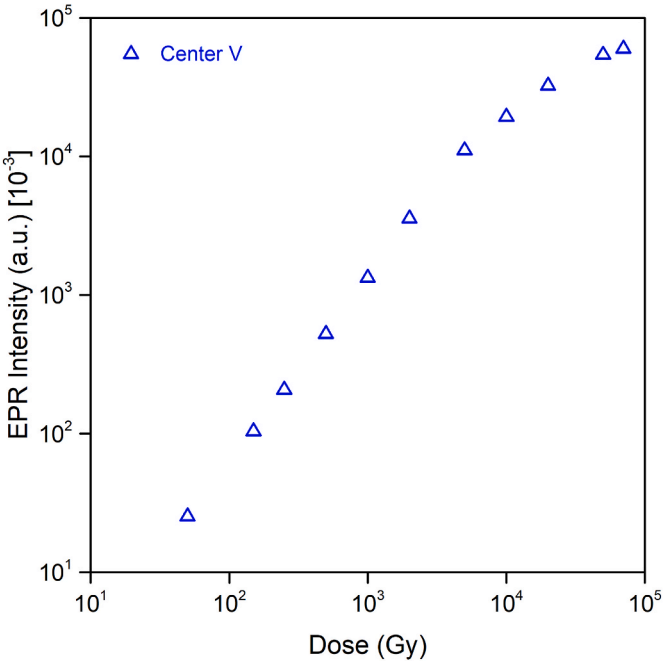

Fig. 9. Dose response curve of center V irradiated with gamma ray between 50 Gy and 70 kGy.

CRediT authorship contribution statement

Nilo F. Cano: Formal analysis, Investigation, Measurements, Writing - original draft, Writing - review & editing, Visualization. **Jorge S. Ayala Arenas:** Methodology, Formal analysis, Investigation, Visualization, Validation. **S. Watanabe:** Methodology, Funding acquisition.

Declaration of competing interest

The authors declare that they have no known competing financial interests or personal relationships that could have appeared to influence the work reported in this paper.

Acknowledgments

The authors would like to express thanks to Ms. E. Somessari from the Institute for Energy and Nuclear Researches (IPEN), Brazil, for kindly carrying out the γ irradiation of the samples. This work was carried out with partial financial support from FAPESP (Fundação de Amparo à Pesquisa do Estado de São Paulo), Brazil (Process number 2014/03085-0). This work was partially supported by CONCYTEC-FONDECYT, Peru, in the framework of the call E038-01 (Process number 037-2019).

References

Acar, A.O., Polat, M., Aydin, T., Aydaş, C., 2016. The ESR dosimetric features of strontium sulfate and temperature effects on radiation-induced signals. Radiat. Phys. Chem. 123, 31–36. https://doi.org/10.1016/j.radphyschem.2016.02.010.

Alzimami, K.S., Maghraby, A.M., Bradley, D.A., 2014. Comparative study of some new EPR dosimeters. Radiat. Phys. Chem. 95, 109–112. https://doi.org/10.1016/j.radphyschem.2012.12.039.

Baffa, O., Kinoshita, A., 2014. Clinical applications of alanine/electron spin resonance dosimetry. Radiat. Environ. Biophys. 53, 233–240. https://doi.org/10.1007/s00411-013-0509-2.

Barbosa, R.F., Cano, N.F., Watanabe, S., Guttler, R.A.S., Reichmann, F., 2014. Thermoluminescence in two varieties of jadeite: irradiation effects and application to high dose dosimetry. Radiat. Meas. 71, 36–38. https://doi.org/10.1016/j.radmeas.2014.05.002.

Belahmar, A., Mikou, M., Saidou, A.M., Baydaoui, E., Bougteb, M., 2018. EPR study of dosimetric properties of glucose irradiated by X-photons and electrons: analyse of storage effect on produced free radicals. Radiat. Phys. Chem. 152, 6–11. https://doi.org/10.1016/j.radphyschem.2018.07.010.

Bortolin, E., Onori, S., 2005. Features of EPR dosimetry with $CaSO_4$:Dy phosphor. Appl. Radiat. Isot. 62, 349–352. https://doi.org/10.1016/j.apradiso.2004.08.024.

Bradshaw, W.W., Cadena, D.G., Crawford, G.W., Spetzler, H.A.W., 1962. The use of alanine as a solid dosimeter. Radiat. Res. 17, 11–21. https://www.jstor.org/stable/3571206.

Cano, N.F., Watanabe, S., Blak, A.R., Yauri, J.M., 2008. Radiation effects on TL and EPR of sodalite and application to dosimetry. J. Phys. Conf. Ser. 249, 24–29. https://doi.org/10.1088/1742-6596/249/1/012022.

Cano, N.F., Ayala-Arenas, J.S., Javier-Ccallata, H.S., Watanabe, S., 2019. OSL and EPR dating of shells and sediments from Congonhas II sambaqui, Santa Catarina, Brazil. Radiat. Phys. Chem. 167, 108240. https://doi.org/10.1016/j.radphyschem.2019.03.044.

Cano, N.F., Gundu Rao, T.K., Silva-Carrera, B.N., Cruz, S.P.S., Javier-Ccallata, H.S., Bedoya-Barriga, Y.A., Ayala-Arenas, J.S., Watanabe, S., 2020. Elucidation of the centers responsible for the TL peaks in the anhydride crystal. J. Lumin. 221, 117082. https://doi.org/10.1016/j.jlumin.2020.117082.

Cano, N.F., Santos, L.H.E., Chubaci, J.F.D., Watanabe, S., 2015. Study of luminescence, color and paramagnetic centers properties of albite. Spectrochim. Acta A 137, 471–476. https://doi.org/10.1016/j.saa.2014.08.085, 2015.

Chen, F., Graeff, C.F.O., Baffa, O., 2007. Response of l-alanine and 2-methylalanine minidosimeters for K-Band (24 GHz) EPR dosimetry. Nucl. Instrum. Methods B 264, 277–281. https://doi.org/10.1016/j.nimb.2007.08.097.

Ciesielski, B., Schultka, K., Kobierska, A., Nowak, R., Peimel-Stuglik, Z., 2003. In vivo alanine/EPR dosimetry in daily clinical practice: a feasibility study. Int. J. Radiat. Oncol. Biol. Phys. 56, 899–905. https://doi.org/10.1016/s0360-3016(03)00196-2.

Gallo, S., Iacoviello, G., Bartolotta, A., Dondi, D., Panzeca, S., Marrale, M., 2017a. ESR dosimeter material properties of phenols compound exposed to radiotherapeutic electron beams. Nucl. Instrum. Methods B 407, 110–117. https://doi.org/10.1016/j.nimb.2017.06.004.

Gallo, S., Iacoviello, G., Panzeca, S., Veronese, I., Bartolotta, A., Dondi, D., Gueli, A.M., Loi, G., Longo, A., Mones, E., Marrale, M., 2017b. Characterization of phenolic pellets for ESR dosimetry in photon beam radiotherapy. Radiat. Environ. Biophys. 56, 471–480. https://doi.org/10.1007/s00411-017-0716-3.

Heydari, M.Z., Malinen, E., Hole, E.O., Sagstuen, E., 2002. Alanine radicals. 2. The composite polycrystalline alanine EPR spectrum studied by ENDOR, thermal annealing, and spectrum simulations. J. Phys. Chem. A 106, 8971–8977. https://pubs.acs.org/doi/abs/10.1021/jp026023c.

Ikeya, M., 1993. New Applications of Electron Spin Resonance: Dating, Dosimetry and Microscopy. World Scientific, Singapore.

Lund, A., Olsson, S., Bonora, M., Lund, E., Gustafsson, H., 2002. New materials for ESR dosimetry. Spectrochim. Acta A. 58, 1301–1311. https://doi.org/10.1016/S1386-1425(01)00719-3.

Lund, E., Gustafsson, H., Danilczuk, M., Sastry, M., Lund, A., Vertad, T., Malinen, E., Hole, E., Sagstuen, E., 2005. Formates and dithionates: sensitive EPR-dosimeter materials for radiation therapy. Appl. Radiat. Isot. 62, 317–324. https://doi.org/10.1016/j.apradiso.2004.08.015.

Malinen, E., Heydari, M.Z., Sagstuen, E., Hole, E.O., 2003a. Alanine radicals, part 3: properties of the components contributing to the EPR spectrum of X-irradiated

alanine dosimeters. Radiat. Res. 159, 23–32. https://doi.org/10.1667/0033-7587(2003)159[0023:ARPPOT]2.0.CO;2.

Malinen, E., Hult, E.A., Hole, E.O., Sagstuen, E., 2003b. Alanine radicals, part 4: relative amounts of radical species in alanine dosimeters after exposure to 6-19 MeV electrons and 10 kV-15 MV photons. Radiat. Res. 159, 149–153. https://doi.org/10.1667/0033-7587(2003)159[0149:ARPRAO]2.0.CO;2.

Marrale, M., Carlino, A., Gallo, S., Longo, A., Panzeca, S., Bolsi, A., Hrbacek, J., Lomax, T., 2016. EPR/alanine dosimetry for two therapeutic proton beams. Nucl. Instrum. Methods B 368, 96–102. https://doi.org/10.1016/j.nimb.2015.12.022.

Marrale, M., Longo, A., Russo, G., Casarino, C., Candiano, G., Gallo, S., Carlino, A., Brai, M., 2015. Dosimetry for electron Intra-Operative Radiotherapy: comparison of output factors obtained through alanine/EPR pellets, ionization chamber and Monte Carlo-GEANT4 simulations for IORT mobile dedicate accelerator. Nucl. Instrum. Methods B 358, 52–58. https://doi.org/10.1016/j.nimb.2015.05.022.

McKeever, S.W.S., Moscovitch, M., Townsend, P.D., 1995. Thermoluminescence Dosimetry Materials: Properties and Uses. Nucl. Tech. Pub., Ashford.

Murali, S., Natarajan, V., Venkataramani, R., Pushparaja Sastry, M.D., 2001. ESR dosimetry using inorganic materials: a case study of Li_2CO_3 and $CaSO_4$:Dy as prospective dosimeters. Appl. Radiat. Isot. 55, 253–258. https://doi.org/10.1016/S0969-8043(01)00043-4.

Nasreddine, A., Kuntz, F., Bitarb, Z.E., 2020. Absorbed dose to water determination for kilo-voltage X-rays using alanine/EPR dosimetry systems. Radiat. Phys. Chem. https://doi.org/10.1016/j.radphyschem.2020.108938.

Olsson, S.K., Lund, E., Lund, A., 2000. Development of ammonium tartrate as an ESR dosimeter material for clinical purposes. Appl. Radiat. Isot. 52, 1235–1242. https://doi.org/10.1016/S0969-8043(00)00077-4.

Onori, S., Bortolin, E., Lavalle, M., Fuochi, P.G., 1998. $CaSO_4$:Dy phosphor as a suitable material for EPR high dose assessment. Radiat. Phys. Chem. 52, 549–553. https://doi.org/10.1016/S0969-806X(98)00093-0.

Preto, P.D., Balraj, V., Dhabekar, B.S., Watanabe, S., Gundu Rao, T.K., Cano, N.F., 2017. Synthesis, thermoluminescence, defect center and dosimetric characteristics of LiF: Mg,Cu,P,Si phosphor. Appl. Radiat. Isot. 130, 21–28. https://doi.org/10.1016/j.apradiso.2017.08.022.

Rushdi, M.A.H., Beshir, B., 2019. EPR dosimetric potential of ammonium oxalate monohydrate in radiation technology. Radiat. Phys. Chem. 162, 121–125. https://doi.org/10.1016/j.radphyschem.2019.05.003.

Sagstuen, E., Hole, E., Haugedal, S., Nelson, W., 1997. Alanine radicals: structure determination by EPR and ENDOR of single crystals X-irradiated at 295 K. J. Phys. Chem. A 101, 9763–9772. https://pubs.acs.org/doi/abs/10.1021/jp972158k.

Smith, C.L., Ankers, E., Best, S.P., Gagliardi, F., Katahira, K., Tsunei, Y., Tominaga, T., Geso, M., 2017. Investigation of IRGANOX®1076 as a dosimeter for clinical X-ray, electron and proton beams and its EPR angular response. Radiat. Phys. Chem. 141, 284–291. https://doi.org/10.1016/j.radphyschem.2017.08.002.

Trompier, F., Fattibene, P., Tikunov, D., Bartolotta, A., Carosi, A., Doca, M.C., 2004. EPR dosimetry in a mixed neutron and gamma radiation field. Radiat. Protect. Dosim. 110 (1–4), 437–442. https://doi.org/10.1093/rpd/nch225. In this issue.

Tuta, C.S., Amiot, M.N., Sommier, L., Ioana, R.M., 2020. Alanine pellets comparison using EPR dosimetry in the frame of quality assurance for a Gamma Knife system in Romania. Radiat. Phys. Chem. 170, 108653. https://doi.org/10.1016/j.radphyschem.2019.108653.

Watanabe, S., Cano, N.F., Carmo, L.S., Barbosa, R.F., Chubaci, J.F.D., 2015a. High- and very-high-dose dosimetry using silicate minerals. Radiat. Meas. 72, 66–69. https://doi.org/10.1016/j.radmeas.2014.11.004.

Watanabe, S., Cano, N.F., Carvalho-Júnior, A.B., Ayala-Arenas, J.S., Gonzales-Lorenzo, C. D., Gundu Rao, T.K., 2019. Dating of carbonate covering cave paintings at Peruaçu, Brazil by TL and EPR methods. Appl. Radiat. Isot. 153, 108847. https://doi.org/10.1016/j.apradiso.2019.108847.

Watanabe, S., Cano, N.F., Gundu Rao, T.K., Oliveira, L.M., Carmo, L.S., Chubaci, J.F.D., 2015b. Radiation dosimetry using decreasing TL intensity in a few variety of silicate crystals. Appl. Radiat. Isot. 105, 119–122. https://doi.org/10.1016/j.apradiso.2015.07.056.

Watanabe, S., Cano, N.F., Gundu Rao, T.K., Silva-Carrera, B.N., Carmo, L.S., Quina, A.J. A., Gennari, R.F., Munita, C.S., Ayala-Arenas, J.S., Fernandes, B.G., 2016. Dating stalagmite from caverna do diabo (Devil'S cave) by TL and EPR techniques. An. Acad. Bras. Ciênc. 88, 2137–2142. https://doi.org/10.1590/0001-3765201620150755.